Jpn. J. Appl. Phys. Vol. 31 (1992) pp. L 1484–L 1487
Part 2, No. 10B, 15 October 1992

Electron Energy-Loss Spectra of Carbon Nanotubes

Ryuichi KUZUO, Masami TERAUCHI and Michiyoshi TANAKA

Research Institute for Scientific Measurements, Tohoku University, Sendai 980

(Received August 17, 1992; accepted for publication August 27, 1992)

Carbon nanotubes were investigated by means of electron energy-loss spectroscopy. Two peaks due to the π plasmon and the $\pi+\sigma$ plasmon were observed. The energy of the $\pi+\sigma$ plasmon peaks varied from 22.0 eV to 24.5 eV, which roughly agrees with the average plasmon energy of graphite. A shoulder due to single electron excitations was observed at 13 eV, which was not observed in graphite. There were two kinds of nanotubes which exhibited their respective π plasmon peaks at 5.2 eV and 6.4 eV. The peaks in the dielectric function obtained by Kramers-Kronig analysis of the spectra were broader than those of graphite probably due to the curving of the graphitic sheets.

KEYWORDS: carbon nanotubes, fullerenes, graphite, EELS, bulk plasmon, interband transition

Since Kroto *et al.*[1] discovered carbon clusters, C_{60} and other fullerenes, great interest has been focused on their crystal structures[2] and electronic properties.[3-5] We investigated C_{60} using electron energy-loss spectroscopy (EELS)[6] and reported that the onset energy at 1.4 eV in the imaginary part ε_2 of the dielectric function is due to the interband transition (band gap) between the highest occupied electronic state and the lowest unoccupied state. The energies of the absorption peaks in ε_2 showed good agreement with those calculated from the band structure.[7]

Recently, Iijima[8] discovered a new form of graphitic carbon needles, called "carbon nanotubes", which are produced by a similar method as that to prepare C_{60} and other fullerenes. Carbon nanotubes are composed of several coaxial cylinders of graphitic sheets, the number of which ranges from 2 to 50. The carbon atom hexagons on a tube are arranged in a helical fashion about the needle axis. Hamada *et al.*[9] have shown from band structure calculations that the electronic structures of carbon nanotubes are categorized as metallic or semiconducting according to their crystal structures. The present paper reports the electron energy-loss spectra of carbon nanotubes and the dielectric function obtained by Kramers-Kronig analysis of the spectra.

Carbon nanotubes used in the present study were supplied by Dr. Y. Saito of Mie Univ., who produced them using the d.c. arc-discharge evaporation method similar to that used for the production of C_{60}. Specimens for electron energy-loss spectroscopy were prepared by dropping a droplet of alcohol containing nanotubes onto microgrids for electron microscopy.

The high-resolution energy-loss spectrometer used was developed as a project of Joint Research with Industry by the Ministry of Education, Science and Culture of Japan.[10,11] The spectrometer was equipped with a thermal-type field emission gun as the electron source and specially designed double-focus Wien filters as the monochromator and the analyzer. As the illumination lens system, the specimen goniometer and the imaging lens system of the spectrometer, the column part of JEM-1200EX was utilized. The electron energy-loss signals were received by the parallel detection system using a charge-coupled device (CCD) camera. The best values of the full widths at the half-maximum (FWHM) of the zero-loss peak at present are 17 meV and 33 meV for cases without and with a specimen, respectively. The accelerating voltage of the incident electron beam was set at 60 keV. The retarding potential of the monochromator was set to be 20 ~ 51 eV, and that of the analyzer was set to be 51 ~ 600 eV. The spectra were measured from areas of 180 nm in diameter during 240 seconds at room temperature. The spectra of nanotubes were measured with rather low resolutions of 0.23 ~ 0.38 eV at the FWHM of the zero-loss peak to obtain sufficient intensity.

Figure 1(a) shows a high-resolution electron microscope image of a carbon nanotube. The nanotube was 31 nm in diameter and consisted of 44 graphitic sheets. Figure 1(b) shows an electron energy-loss spectrum in an energy region from 0 to 50 eV obtained from the carbon nanotube of Fig. 1(a). The energy resolution was 0.31 eV for the FWHM of the zero-loss peak. Two distinct peaks are seen at 6.4 eV and 22.6 eV (arrows). When the loss function of graphite in Fig. 3 is used as a reference, these two peaks are identified as the collective excitation due to the π electrons (π plasmon) and the whole valence electrons ($\pi+\sigma$ plasmon), respectively. There is a shoulder at about 13 eV, which does not appear in the loss function of graphite. The shoulder may be attributed to the $\sigma\rightarrow\sigma^*$, $\sigma\rightarrow\pi^*$ and $\pi\rightarrow\sigma^*$ transitions. The detailed structure of the π plasmon peak will be dealt with later in this paper.

Figure 2(a) shows the loss function ($\mathrm{Im}\,[-1/\varepsilon]$) obtained from the spectrum of Fig. 1(b) by removing the contributions due to multiple scattering of electrons. The intensity of the direct beam was subtracted by a Lorentzian fit. It is noted that the loss function in the region from 0 to 3 eV contains some error due to the ambiguity of the Lorentzian fit. It is common for the absolute value of the loss function to be determined from the condition $\mathrm{Re}\,[-1/\varepsilon(0)]=-1/\varepsilon_1(0)=-1/n^2$, where n is the refractive index. However, since the value of the refractive index of the carbon nanotube is not known, the sumrule[12]

$$\int_0^{\infty}\omega\,\mathrm{Im}\,[-1/\varepsilon(\omega)]\,\mathrm{d}\omega=\frac{\pi}{2}\omega_p^2$$

(a)

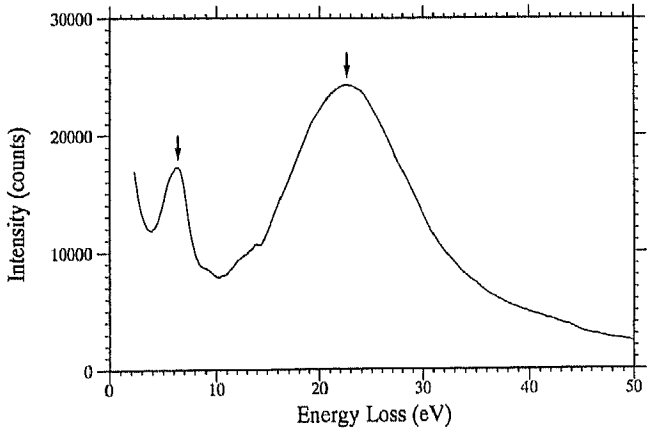

(b)

Fig. 1. (a) High-resolution electron microscope image of a carbon nanotube. (b) Electron energy-loss spectrum of a carbon nanotube in the energy range from 0 to 50 eV. The energy resolution was 0.31 eV. Two bulk plasmon peaks are seen at 6.4 eV and 22.6 eV (arrows).

$$\left(\omega_p = \sqrt{\frac{4\pi N e^2}{m}}\right)$$

was used to determine the absolute value of the loss function, where N is the electron density, e is the electron charge, and m is the rest mass of an electron. The value of ω_p was taken to be 22.6 eV from Fig. 1(b). It should be noted that in cases of graphite and C_{60} the loss function obtained using the sumrule is confirmed to show good agreement with that obtained using the refractive index.

Figures 2(b) and 2(c) show the real part (ε_1) and the imaginary part (ε_2) of the dielectric function, which were ob-

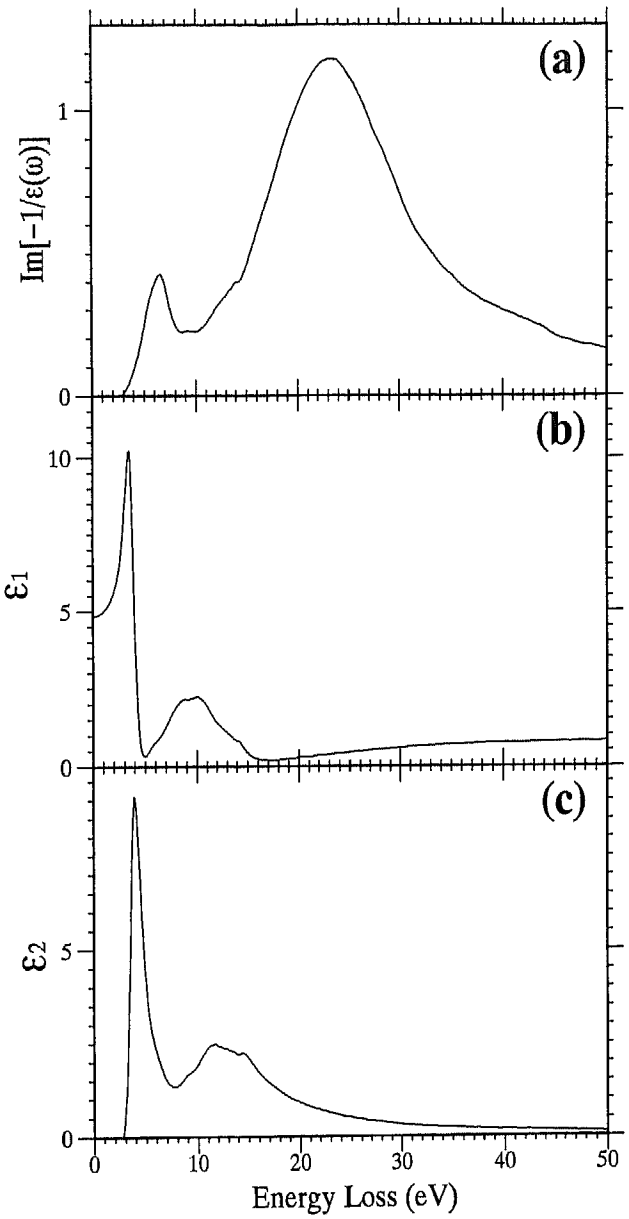

Fig. 2. The loss function (a), the real part (b) and the imaginary part (c) of the dielectric function of a carbon nanotube. The dielectric function was obtained by Kramers-Kronig analysis of the loss function.

tained from Kramers-Kronig analysis (KKA) of the loss function. The integration with respect to energy in KKA was carried out up to 400 eV, where the loss function in a high-energy region was extrapolated using the equation AE^{-b}, b being taken to be 4.0. For comparison, we show in Fig. 3 the loss function and the real and imaginary parts of the dielectric function obtained from a spectrum for graphite which was measured with the electron incidence parallel to the c axis. In the case of graphite, the $\pi \rightarrow \pi^*$ transition at 4 eV in ε_2 causes the π plasmon peak at 7 eV in the loss function. Hence, the peak at 4 eV in ε_2 of the carbon nanotube is also assigned to the $\pi \rightarrow \pi^*$ transition. The broad peak at 12 ~ 14 eV in ε_2 of the carbon nanotube is assigned to the $\sigma \rightarrow \sigma^*$, $\sigma \rightarrow \pi^*$ and $\pi \rightarrow \sigma^*$ transitions by reference to the corresponding curve of graphite. The peak is much broader than that of

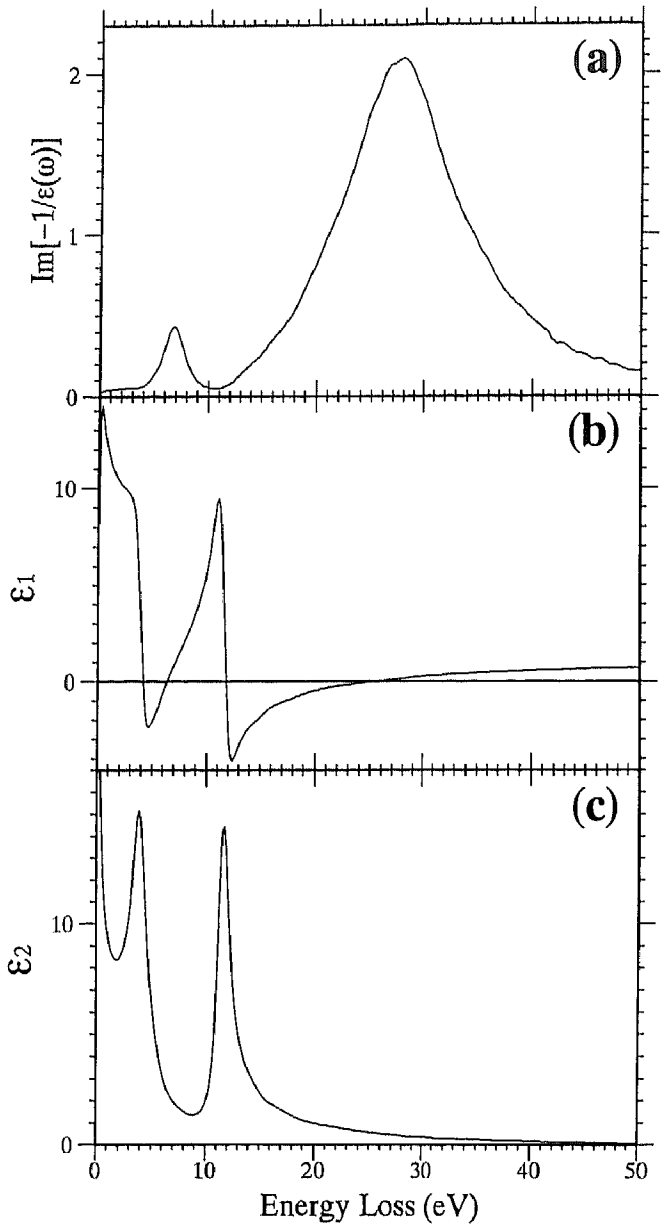

Fig. 3. The loss function and the dielectric function of graphite.

graphite. This may be attributed to the removal of the degeneracy of the π electron energy states due to the curving of graphitic sheets in the nanotube.

The $\pi+\sigma$ plasmon peak in the loss spectrum of the carbon nanotube appears at an energy of about 5 eV lower than that of graphite measured with the electron incidence parallel to the c axis. This suggests that the electron density of the carbon nanotube is less than that of graphite. To interpret this difference, the electron density of the carbon nanotube must be 32% less than that of graphite. However, the electron density of the carbon nanotube is considered to differ only slightly, because Iijima[8] reported that the distance between the graphitic sheets in the nanotube is nearly the same as that of graphite. Another possibility to explain the difference may be the difference of the relaxation time between two plasmons, because the plasmon peak is shifted to a lower energy when the effect of the relaxation time is taken into account.[13] However, the difference of the FWHM values of the plasmon peaks in graphite (13 eV) and the carbon nanotube (16 eV) causes only 0.5 eV of the difference of the energy shift. It is known that the loss spectrum of graphite depends on the direction of the wave number vector of loss electrons. The plasmon energy of graphite measured with the wave number vector set parallel to the c axis is about 20 eV, which is 7 eV less than that measured with the wave number vector set perpendicular to the c axis.[14] Since the graphitic sheets of the carbon nanotube form cylinders, they are illuminated by incident electrons with the parallel and perpendicular settings at the same time. Therefore, the plasmon energy of the carbon nanotube should be compared with the mean value of the plasmon energies measured at the two settings of graphite. The mean value of the plasmon energies of graphite is about 23.5 eV. The value roughly agrees with that of the carbon nanotube.

Figure 4 shows C1s absorption spectra of the carbon nanotube and graphite. The energy resolution was 0.38 eV for the FWHM of the zero-loss peak. The C1s absorption spectrum of the nanotube is similar to that of graphite; transitions from 1s to the unoccupied π^* level and to the unoccupied σ^* level are seen at 286 eV and 292 eV, respectively, in both figures. The fact that the $1s\rightarrow\pi^*$ transition peak of the carbon nanotube is slightly broader than that of graphite may again be explained by the broadening of the π^* states in the curved graphitic sheets.

Figure 5 shows the electron energy-loss spectra in an energy range from 0 to 15 eV obtained from carbon nanotube A, which is the same one as shown in Fig. 1(a), and from carbon nanotube B whose diameter is 13 nm. The energy resolution is 0.23 eV. The π plasmon peak at 6.4 eV in carbon nanotube A (arrow) is accompanied by a shoulder at 5.2 eV (vertical line). On the other hand, a peak at 5.2 eV (arrow) with a shoulder at 6.4 eV (vertical line) is seen for carbon nanotube B. Table I summarizes

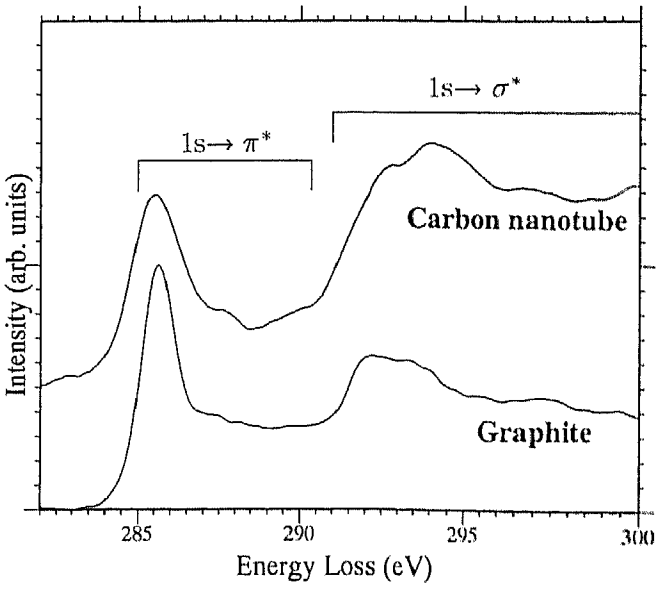

Fig. 4. Electron energy-loss spectra of a carbon nanotube and graphite in the energy range from 282 to 300 eV. The energy resolution was 0.38 eV.

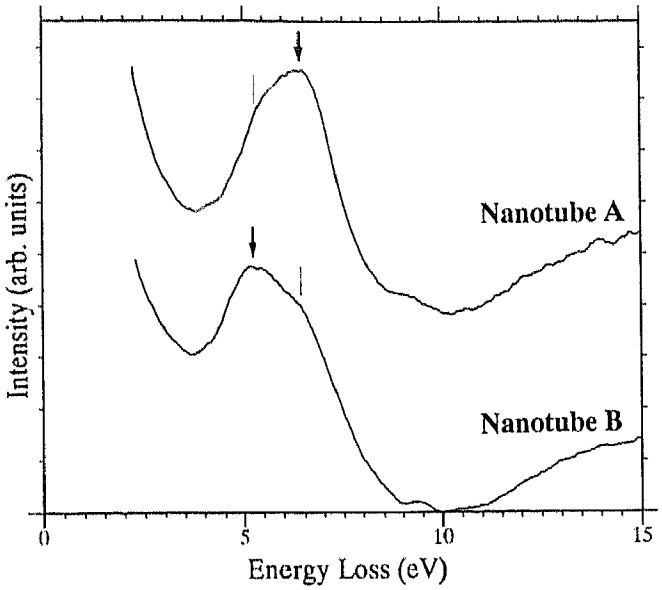

Fig. 5. Electron energy-loss spectra of carbon nanotubes A and B in the energy range from 0 to 15 eV. The energy resolution was 0.23 eV.

Table 1. The diameters and the numbers of sheets were measured from high-resolution electron microscope images. The energies of the plasmon peaks were obtained from electron energy-loss spectra. The mark *) means that spectra were measured from two nanotubes overlapped in the direction of the electron incidence.

Nanotube no.	Diameter (nm)	Number of sheets	π plasmon energy (eV)	$\pi+\sigma$ plasmon energy (eV)
1	15	21	5.4	22.7
2 (A)	31	44	6.4	22.6
3	20	26	6.2	22.0
4 (B)	13	—	5.2	23.7
5	17	—	5.4	24.5
6*)	31, 34	—	6.3	24.1
7*)	14, 13	—	5.1	23.1
8*)	20, 14	—	6.2	24.1

the plasmon peak energies of eight nanotubes which we measured. Four nanotubes (Nos. 2, 3, 6, 8) showed the spectra like that of nanotube A (type A) and the other four (Nos. 1, 4, 5, 7) showed the spectra like that of nanotube B (type B). Carbon nanotubes which have small diameters less than about 20 nm showed type B spectra. On the other hand, the $\pi+\sigma$ plasmon energies of the nanotubes ranged from 22.0 to 24.5 eV. No special relationship was found between the values of the $\pi+\sigma$ plasmon and the diameters of the nanotubes.

It is hoped that electron energy-loss spectra will be measured for a larger number of carbon nanotubes in order to reveal with certainty the correlation between the loss spectra and the sizes of nanotubes.

Acknowledgements

The authors thank Dr. Y. Saito of Mie Univ. for supplying the nanotubes. Thanks are also due to Mr. Y. Harada, Dr. K. Tsuno and Mr. J. Ohyama of JEOL for their great effort in constructing the EELS instrument. The present work was mainly supported by a project of Joint Research with Industry by the Ministry of Education, Science and Culture.

References

1) H. W. Kroto, J. R. Heath, S. C. O'Brien, R. F. Curl and R. E. Smalley: Nature **318** (1985) 162.
2) R. M. Fleming, T. Siegrist, P. Marsh, B. Hessen, A. R. Kortan, D. W. Murphy, R. C. Haddon, R. Tycko, G. Dabbagh, A. M. Mujsce, M. L. Kaplan and S. M. Zahurak: Mater. Res. Soc. Symp. Proc. **206** (1991) 691.
3) A. F. Hebard, M. J. Rosseinsky, R. C. Haddon, D. W. Murphy, S. H. Glarum, T. M. Palstra, A. P. Ramirez and A. R. Kortan: Nature **350** (1991) 60.
4) M. J. Rosseinsky, A. P. Ramirez, S. H. Glarum, D. W. Murphy, R. C. Haddon, A. F. Hebard, T. M. Palstra, A. R. Kortan, S. M. Zahurak and A. V. Makhija: Phys. Rev. Lett. **66** (1991) 2830.
5) K. Holczer, O. Klein, S. M. Huang, R. B. Kaner, K. J. Fu, R. L. Whetten and F. Diederich: Science **252** (1991) 1154.
6) R. Kuzuo, M. Terauchi, M. Tanaka, Y. Saito and H. Shinohara: Jpn. J. Appl. Phys. **30** (1991) 1817.
7) S. Saito and A. Oshiyama: Phys. Rev. Lett. **66** (1991) 2637.
8) S. Iijima: Nature **354** (1991) 56.
9) N. Hamada, S. Sawada and A. Oshiyama: Phys. Rev. Lett. **68** (1992) 1579.
10) K. Tsuno, M. Terauchi and M. Tanaka: Optik **83** (1988) 77.
11) M. Terauchi, R. Kuzuo, F. Satou, M. Tanaka, K. Tsuno and J. Ohyama: *Proc. Int. Congress for Electron Microscopy* (San Francisco Press, San Francisco, 1990).
12) H. Raether: *Excitation of Plasmons and Interband Transitions by Electrons* (Springer, Berlin, Heidelberg, New York, 1980) Springer Tract in Modern Physics Vol. 88.
13) R. F. Egerton: *Electron Energy Loss Spectroscopy in the Electron Microscope* (Plenum Press, New York & London, 1986).
14) H. Venghaus: Phys. Status Solidi b **71** (1975) 609.